ISSN: 0976-3031

Available Online at http://www.recentscientific.com

CODEN: IJRSFP (USA)

International Journal of Recent Scientific Research
Vol. 8, Issue, 7, pp. 18869-18873, July, 2017

International Journal of Recent Scientific Research

DOI: 10.24327/IJRSR

Research Article

DESIGN AND ANALYSIS OF PZT-6 TONPILZ TRANSDUCER

Anu and Ritu

Department of ECE, GJU&ST. Hisar

DOI: http://dx.doi.org/10.24327/ijrsr.2017.0807.0583

ARTICLE INFO

Article History:

Received 15th April, 2017
Received in revised form 25th May, 2017
Accepted 23rd June, 2017
Published online 28th July, 2017

Key Words:

PZT-6, Tonpilz Transducer, TVR, SPL

ABSTRACT

In this paper a Tonpilz transducer has been designed and analysed. This transducer consists of 6 piezoceramic rings stacked between an aluminum head mass and a steel tail mass connected by a steel bolt. The head mass is exposed to an unbounded region of water and a Perfectly Matched Layer is used to model the absorption of sound waves as they propagate far away from the sound source. The model designed using finite element method has been studied for Transmitting Voltage Response, Sound Pressure Level, Acoustic Impedance and Total Structural Displacement in the frequency range of 1-70 khz. This design has given the Sound Pressure Level of 208 db, Radiated Pressure Field of 64 Mpa and Transmitting Voltage Response 155 db at the frequency of 50 khz.

Copyright © Anu and Ritu, 2017, this is an open-access article distributed under the terms of the Creative Commons Attribution License, which permits unrestricted use, distribution and reproduction in any medium, provided the original work is properly cited.

INTRODUCTION

Underwater acoustic communication is a hot research topic now days, so the transducer of high Transmitting Voltage Response had been designed. The Tonpilz (sound mushroom) transducer is a relatively low frequency, high power sound emission transducer [5]. So it is one of the popular transducer designs that are used for SONAR [1-2]. It is often referred as a piston transducer as the radiating face ideally vibrates uniformly in a piston like motion [2]. Tonpilz transducers have high value of TVR so they are typically designed to be an efficient projector.

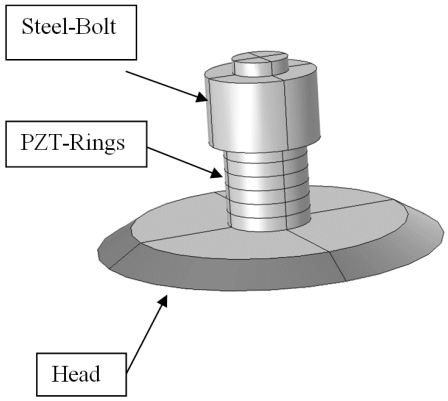

Figure 1 A Tonpilz transducer.

They are commercially available in a wide range of bandwidths and are therefore well-suited for a various applications [6] Such as collision avoidance, communication, ultrasonic imaging. As shown in figure 1, Tonpilz transducers [3] tend to have many components, thus their manufacturing is complex, especially when attempting to make small devices. The design and analysis has been done using Finite Element Method (FEM) [9].In this design lead zirconate titanate (**PZT**) material is used for its precision positioning. Bolt of the transducer are made up of steel material. In addition, head of aluminium is generally used. The speed of sound in all medium is different such as in water speed of sound 1484m/s speed of sound in air is 343m/s, in solid is 5120m/s. In this transducer every piezo disks are excited with a 5v RMS ELECTRICAL SIGNAL. . A Perfectly Matched Layer (PML) is used to model the absorption of sound waves as they propagate far away from the sound source. Here for good TVR ideal water of 1000 kg/m^3 is taken. The finite element method uses a three dimensional representation of the transducers governing equations and so has none of the limitations of 1-D modelling[12].This work attempt to improve the TVR of the Tonpilz transducer. One drawback of this design is number of the PZT rings.

Model Definition

The Tonpilz transducer modeled in this paper consists of 6 piezoceramic rings stacked between an aluminum head mass and a steel tail mass connected by a steel bolt [4]. This central bolt could be pre-stressed to control the transducer response.

Corresponding author:* **Anu
Department of ECE, GJU&ST. Hisar

In this design, the effect of pre-stress in the bolt is not considered. The tail and head mass are used to lower the resonance frequency of the device to the desired level. The Piezo devices made of lead zirconate titanate (**PZT**) [8] are capable of driving mechanical devices for precision positioning.

Table 1 Properties of Materials.

Material	Density	Young's Modules	Poisson Ratio
Aluminium	2700 kg/m^3	70 GPa	0.33
Steel	7850 kg/m^3	205 GPa	0.28
PZT	7500 kg/m^3	63 GPa	0.31

The outer curved surface of the steel tail mass is assumed to be fixed. Each of the piezo disks are excited with a 5 V RMS electrical signal. The design determines the deformation in the device, the radiated pressure field and sound pressure level, as well as the spatial far-field sensitivity, the transmitting voltage response (TVR) curve of the transducer and the frequency range of 1 kHz to 70 kHz, which are divided into 60 divisions. The head mass is exposed to an unbounded region of water. A Perfectly Matched Layer (PML) is used to model the absorption of sound waves as they propagate far away from the sound source. Note that the modelling geometry has a rotational symmetry, using a full 3D geometry allows us to capture any vibration mode of the transducer and acoustic mode of the fluid region that do not possess such a symmetry in the solution. Figure 2 shows an axis semetric view of the actual 3D model.

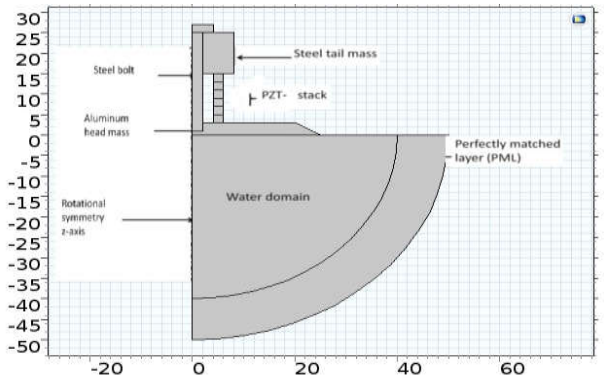

Figure 2 An axis semetric section of the model geometry.

Physics Implementation

The Acoustic-Piezoelectric Interaction, Frequency Domain multi physics interface available in the Acoustics Module is used for simulating the multi physics interactions. This predefined interface includes the necessary fundamental physics which are Pressure Acoustics, Solid Mechanics and Electrostatics. The Pressure Acoustics interface is used to solve for the wave equation in the water domain. The Solid Mechanics physics is solved on all structural materials including the PZT-6 disks. The Electrostatics physics is solved on the PZT-6 disks. The multi physics couplings necessary to model this system are available as predefined nodes under the Multi physics branch [11]. These couplings are:

***Acoustic-Structure Boundary*:** This node is active on the boundaries that are at the interface of the water domain and transducer head mass. On these boundaries a bidirectional coupling is automatically set up. The fluid pressure evaluated by the Pressure Acoustics physics is applied as a mechanical load in the Solid Mechanics physics. Furthermore, the normal component of the structural acceleration is used as a sound source.

***Piezoelectric Effect*:** This node is active on the PZT-6 domains only and couple the Solid Mechanics and Electrostatics equations solved in these domains via the linear constitutive equations that model the piezoelectric effect by coupling stresses and strains with electric field and electric displacement.

Transducer Characteristics

The frequency response of the following important transducer characteristics are investigated in this paper.

Specific Acoustic Impedance

The specific acoustic impedance Zaco is computed as the ratio of the impedance of the head mass surface exposed to water to the characteristic impedance Z_0 of water as shown in Eq 1. The value of Z_0 is computed from the product of density and speed of sound in water at a temperature of 293.15 K.

$$Z_{aco} = \frac{\int pda / \int v_{nda}}{Z_0} \quad (1)$$

P= acoustic pressure
Da= change in the area
Z_0=Impudence
Z_{aco}=acoustic impudence

The impedance of the head mass surface is computed from the ratio of the area integral of the acoustic pressure p to the area integral (da) of the normal component of the structural velocity v_n of the surface. In this case the normal velocity is the same as the Z-component of the velocity *v*z, so we can say vn is vz and which in frequency domain can be represented as the product of the Z-component of the structural displacement w, the variable j which is the imaginary number square root of -1 and the angular frequency of vibration ω. The area integral is computed by introducing an integration coupling operator that is assigned to the surface of interest.

Transmitting Voltage Response (TVR)

The TVR represents the sensitivity of the transducer measured at a distance of 1 m and driven at 5 V RMS. This definition can be mathematically expressed using Eq 2 where Prms is RMS pressure at 1m and Vrms is RMS voltage.

$$\text{TVR} = 20log\frac{Prms/V_{rms}}{1\mu pav^{-1}} \quad (2)$$

P_{RMS}=Rms value of pressure
V_{RMS}=Rms value of voltage

Sound pressure level or acoustic pressure level is a logarithmic measure of the effective pressure of a sound relative to a reference value.

Sound pressure level SPL, is defined by Eq.(3):

$$SPL = 20\ log \frac{P_{rms}}{P_{ref}} \quad (3)$$

Sound power or acoustic power is the rate at which sound energy is emitted, reflected, transmitted or received, per unit time. Sound power is defined as Eq (4)

P = f.v = Apu.v =Apv (4)
A=Area
P=Sound pressure
F= Sound force of unit vector v

RESULT

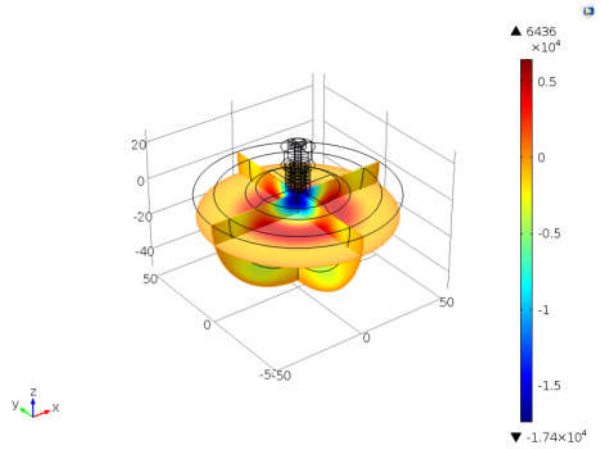

Figure 3 A multi slice plot showing the total acoustic pressure variation in the water domain and PML at 50 kHz.

Figure 3 shows the total acoustic pressure in the water domain for 50 kHz excitation which is the 41st division of the bandwidth. Maximum value is shown by red colour and the value is 64.36 MPa.

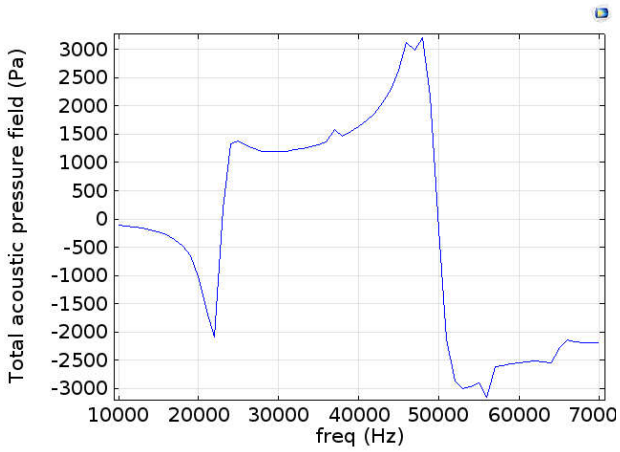

Figure 4 The total acoustic pressure

Figure 4 shows the total acoustic pressure. From the figure it can be seen that at frequencies 22 kHz and 50 kHz there is a dip from higher value to lower vale of pressure. Larger the dip or different in the total acoustic pressure will give us resonant frequencies.

Figure 5 shows the sound pressure level (SPL) in the water domain for 50 kHz excitation. Note the 50 dB difference between the SPL near the transducer head mass and the outer surface of the PML layer. This once again confirms the effectiveness of the damping induced by the PML.

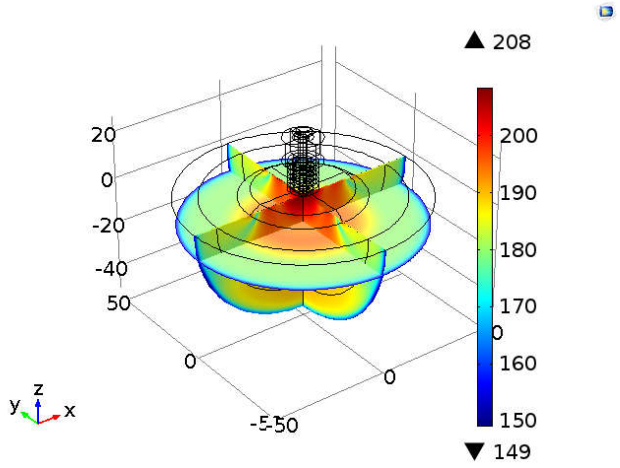

Figure 5 A multi slice plot showing the sound pressure level (SPL) in the water domain and PML at 50 kHz.

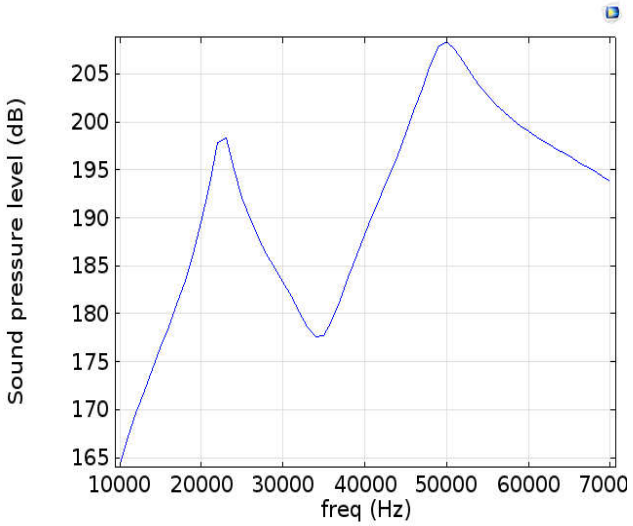

Figure 6 Sound Pressure Level.

Figure 6 shows the SPL curve in this graph it is clear that at resonant frequency there is a peak in SPL which are clearly seen at 22 kHz and 50 kHz and maximum value is 198 dB and 208 dB respectively.

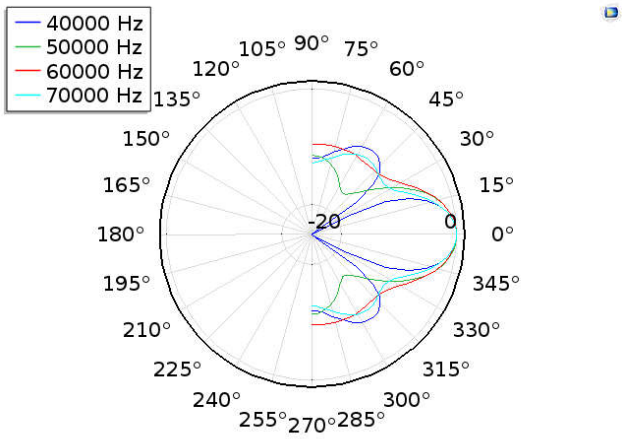

Figure 7 A polar beam sensitivity plot showing the sound pressure level (SPL).

Figure 7 shows a polar beam sensitivity plot which is also known as the beam pattern. Here the relative far-field SPL is computed at a radial distance of 10 m from the transducer head mass for 40, 50, 60 and 70 kHz excitation. The polar plot here shows the radiation pattern in the XZ-plane.

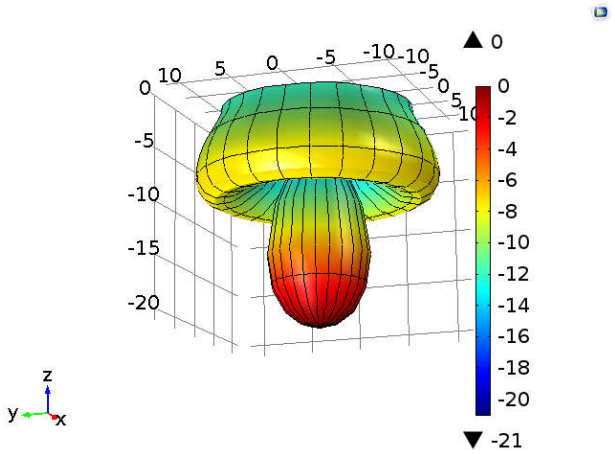

Figure 8 A 3D far field plot showing the sound pressure level (SPL).

Figure 8 shows a 3D polar plot of the far field SPL computed at a radial distance of 10 m from the transducer head mass for 50 kHz excitation. It can be seen that the main lobe is three times bigger than the side lobes. The SPL shown here is computed relative to a value of 0 dB at an on-axis distance of 10 m direct ahead of the transducer head mass.

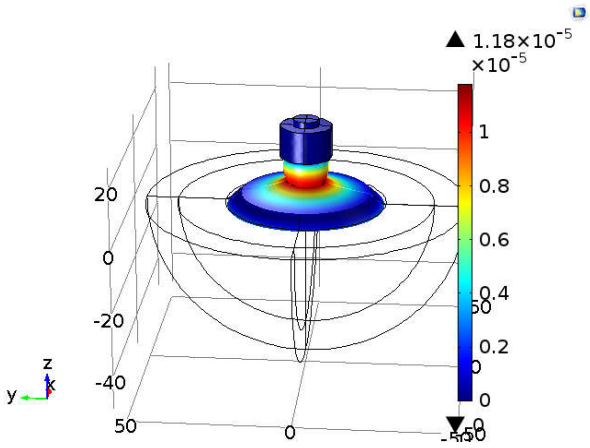

Figure 9 Total structural displacement of the transducer at 50 kHz.

Figure 9 shows the total structural displacement of the tonpilz transducer at 50 kHz excitation. At this frequency, the head mass vibrates in a mode whose shape is some what toroidal. This produces the lobes in the sound radiation pattern

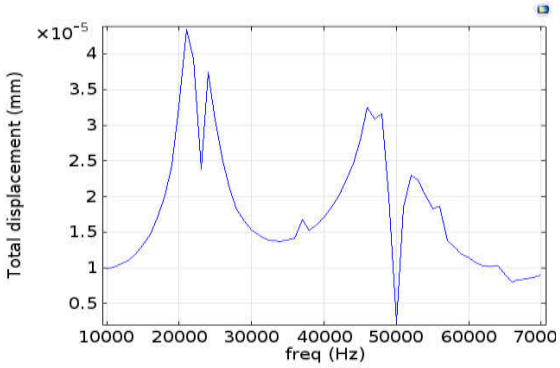

Figure 10 Total structural displacement of the transducer

There is Sharpe dip at resonant frequencies in displacement shown by figure 10. It is concluded that there will be minimum energy loss at these frequencies and all the energy is transferred in water.

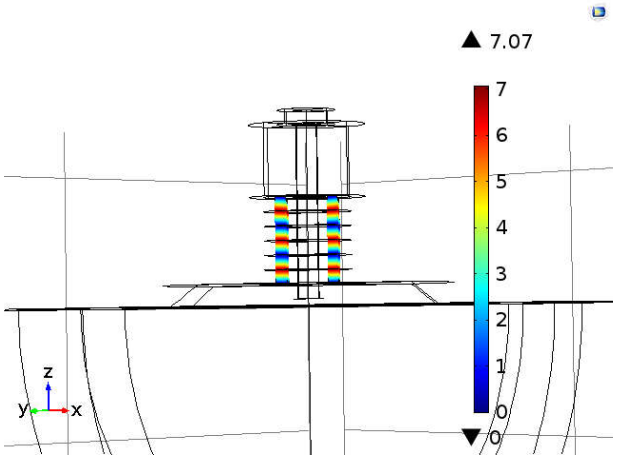

Figure 11 A multi slice plot of the electric potential distribution within the PZT-6 disks.

Figure 11 zooms on the piezo stacks. It shows the electric potential distribution through the thickness of the PZT-6 disks. It will be same for all the frequencies.

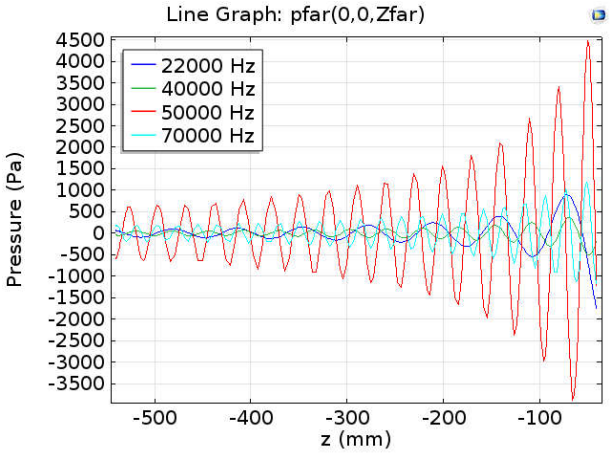

Figure 12 A line plot of sound pressure variation directly ahead of the transducer head mass up to an on-axis distance of 500 mm.

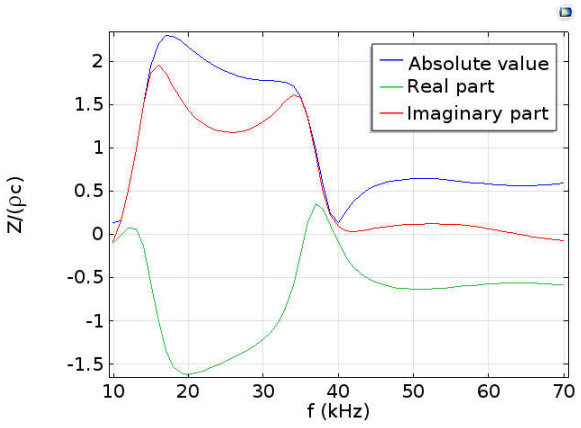

Figure 13 Frequency response plot of the absolute value, real and imaginary components of the specific acoustic impedance at the interface between the head mass and water.

Figure 12 shows a plot of acoustic pressure vs. Z-coordinate along the axis of the transducer for an excitation frequency of 22, 40, 50 and70 kHz. At 50 KHz the sound waves are produce of high intensity as compared to the others, thus at 50KHz the sound waves travels the maximum distance.

Figure 13 shows the frequency response of the specific acoustic impedance of the head mass surface that is exposed to water. Impedance is very stable in PZT after 40 kHz frequencies as compared at low frequencies.

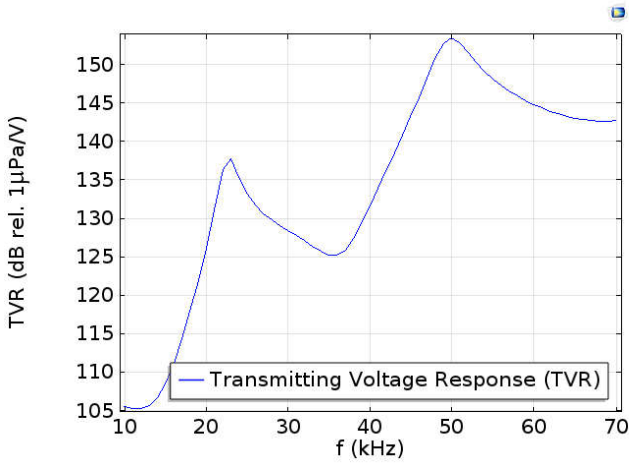

Figure 14 Transmitting Voltage Response (TVR) as a function of frequency

Figure 14 shows the variation in the TVR of the transducer as a function of operating frequency obtained in the direction of the wave at an on-axis distance of 1 m ahead of the head mass and computed relative to 1 µPa/V. Maximum the value of TVR greater is the performance thus it works best at 50 KHz and is given by 208dB. At 22kHz also there is a peak but value of 50kHz is more.

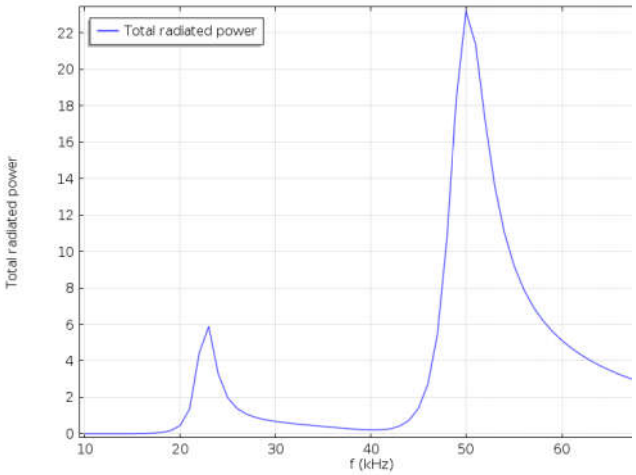

Figure 15 Total radiated power from the tonpilz transducer.

Figure 15 shows the total radiated power as a function of the operating frequency of the tonpilz transducer. Note that the acoustic radiated power should be always positive. The peaks of total radiated power are also at 22kHz and 50 kHz.

The best operating frequency for this design is 50KHz. At this frequency the distance traveled by wave, TVR, TRP and SPL all has the maximum vales.

CONCLUSION

In this paper, a tonpilz transducer for underwater acoustics is successfully developed and analysed. The head design plays an important role in characterizing the performance of a transducer. The head-mass, material and diameter was seen to be a key determinant of the resonant frequency. IT is found that the directional properties of a transducer with an air-gap to be better than without an air-gap. The transducer properties are fairly constant upon miniaturization., it is possible also to do a study on performance variability, which can be useful in developing uniform and identical transducers. In the future the dimensions of the transducer can also be designed and analysed.

References

1. Prashant Kumar, P Priyadarshini, “Underwater acoustic sensor network for early warning generation”. *In: Oceans,* IEEE, pp. 1-6, 2012.
2. C. H. Sherman and J. L. Butler, “Transducers and Arrays for Underwater Sound”, Springer, New York, pp. 543-609, 2007.
3. Qifa Zhou, Jonathan M. Cannata, “Fabrication and Characterization of Micromachined High-Frequency Tonpilz Transducers Derived by PZT Thick Films”, IEEE Transactions on Ultrasonics, ferroelectrics, and frequency control, vol. 52(), no. 3, pp. 350-357, 2005.
4. Filmichard J. Meyer, Jr., Thomas C. Montgomery, and W. Jack Hughes, “Tonpilz Transducers Designed Using Single Crystal Piezoelectrics”, IEEE, vol.4, pp.2328-2333, 2002.
5. Qingshan Yao and Leif Bjgrng, “Broadband Tonpilz Underwater Acoustic Transducers based on multimode optimization”, IEEE Transactions on Ultrasonics, Ferroelectrics, and Frequency Control, vol. 44, pp. 5, 1997.
6. M. Lasky, “Review of Undersea Acoustics to 1950,” J. Acoust. Soc. Am., vol. 61, pp.283-297, 1976.
7. D. T. Blackstock, “Fundamentals of Physical Acoustics,” John Wiley & Sons, pp.568, 2000.
8. Rödel, J., Webber, K. G., Dittmer, R., Jo, W., Kimura, M., & Damjanovic, D, “Transferring lead-free piezoelectric ceramics into application”, *J. Europ. Ceram. Soc.*, vol.35, pp.1659-1681, 2015.
9. ATILA, Finite-Element soft. package for the analysis of 2D & 3D structures based on smart materials, version 6.0.2 User’s manual, 2010.
10. Krimholtz, R., Leedom, D., Matthaei, G., “New equivalent circuits for elementary piezoelectric transducers”, *Elec. Letters,* vol. 3, no.13, pp. 398-399, 1970.
11. Publication and proposed revision of ANSI/IEEE standard 176-1987, IEEE trans. Ultras, Ferro, Freq. Contr., 43:717, 1996.
12. 0. C. Zienkiewicz and R. L. Taylor, The Finite Element Merhod: Volumes I and U, 4th ed. London: McGraw-Hill, 1989